Discontinuous GBSAR deformation monitoring

Michele Crosetto[1], Oriol Monserrat, Guido Luzi, María Cuevas-González, Núria Devanthéry

Institute of Geomatics, Parc Mediterrani de la Tecnologia, E-08860 Castelldefels, Barcelona, Spain

Abstract

This paper is focused on deformation monitoring using the Ground-Based SAR (GBSAR) technique and a particular data acquisition configuration, which is called discontinuous GBSAR (D-GBSAR). In the most commonly used GBSAR configuration, the radar is left installed in situ, acquiring data periodically, e.g. every few minutes. Deformations are estimated by processing sets of GBSAR images acquired during several weeks or months, without moving the system. By contrast, in the D-GBSAR the radar is installed and dismounted at each measurement campaign, revisiting a given site periodically. This configuration is useful to monitor slow deformation phenomena. This paper outlines the D-GBSAR data processing and analysis procedure implemented by the authors. This is followed by a discussion of some specific aspects of D-GBSAR monitoring, which concern the density of the deformation measurements, the phase unwrapping, and the estimation of the atmospheric effects. Two successful examples of D-GBSAR deformation monitoring are analysed and discussed: one concerns an urban area, while the second one involves a rural area where the deformation monitoring requires the use of artificial corner reflectors.

Keywords: SAR, GBSAR, Deformation monitoring, Landslides.

1. Introduction

Ground-Based SAR (GBSAR) interferometry is a radar-based terrestrial remote sensing technique (Tarchi et al., 1999), which can be used for digital elevation model generation or

[1] Corresponding author: Michele Crosetto, Institute of Geomatics, Parc Mediterrani de la Tecnologia, Av. Gauss 11, E-08860 Castelldefels, Barcelona, Spain. Email: michele.crosetto@ideg.es; Tel.: +34935569294; Fax: +34935569292.

deformation monitoring (Monserrat et al., 2014). This paper is focused on the latter application. GBSAR deformation monitoring can be performed using two types of acquisition modes: the continuous (C-GBSAR) and the discontinuous (D-GBSAR). In the C-GBSAR the radar is left installed in situ, acquiring data periodically, with a period that typically ranges from a few minutes to a few hours. This is the most commonly used configuration, which can provide a near real-time deformation monitoring (Casagli et al., 2003; Tarchi et al., 2003a; Tarchi et al., 2005) and which offers the best performances in terms of density, precision and reliability of deformation measurements (Monserrat et al., 2014). The most relevant C-GBSAR applications include slope monitoring in open pit mines for operational early warning systems (Noon et al., 2007; Mecatti et al., 2010; Farina et al., 2012); slope instability monitoring related to rockslides (Tarchi et al., 2005), landslides (Tarchi et al., 2003b; Luzi et al., 2006; Barla et al., 2010) or volcanoes (Casagli et al. 2010); urban monitoring (Pieraccini et al., 2004; Pipia et al., 2013); structure monitoring (Tarchi et al., 1997); dam monitoring (Tarchi et al., 1999); dike monitoring (Monserrat, 2012); and glacier monitoring (Noferini et al., 2009; Strozzi et al., 2012).

In the D-GBSAR configuration the radar is installed and dismounted at each campaign, revisiting a given site periodically, e.g. monthly, yearly, etc. depending on the kinematics of the deformation phenomenon at hand and the monitoring requirements. This configuration, which is useful to monitor slow deformation phenomena, is usually adopted by many other deformation monitoring techniques. Its main advantage is the reduced monitoring cost by using the same instrument over several sites. Its drawbacks include a more complex data processing and, generally speaking, reduced density, precision and reliability of deformation measurements. In the literature there are only a few works that describe D-GBSAR applications, e.g. see Noferini et al. (2008), Luzi et al. (2010) and Wujanz et al. (2013).

The paper starts with a discussion of the specific aspects of the D-GBSAR processing chain implemented by the authors. This is followed by the description of a D-GBSAR deformation

monitoring of an urban area: the village of Barberà de la Conca (Catalonia, Spain). Then a more complex example is illustrated, which concerns a rural area close to the village of Canillo (Andorra). In this case the monitoring was performed using artificial Corner Reflectors (CRs). Both case studies were monitored using a Ku-band GBSAR: the IBIS-L by IDS Spa (www.idscorporation.com). Finally, the conclusions summarize the main results of this work.

2. D-GBSAR data processing and analysis

This section outlines the D-GBSAR data processing procedure implemented by the authors. It has several points in common with the processing chain used with C-GBSAR data. In addition, both processing chains share common tools with the procedure to process satellite-based SAR interferometric data. The flow chart of D-GBSAR data processing and analysis procedure is shown in Figure 1, see Monserrat (2012) and Monserrat et al. (2014). The flow chart assumes that N images are acquired, typically at N different campaigns. These images are firstly focused and co-registered. This is followed by the generation of N-1 interferograms and the associated coherence images. Using these images or, alternatively, the so-called Dispersion of Amplitude (the ratio between the standard deviation and the mean of image amplitudes, see Ferretti et al, (2001)), a pixel selection is performed, which aims at separating the pixels that contain information (deformation measurements) from those that are dominated by noise and do not carry any information and hence need to be rejected. A spatial phase unwrapping is performed on the selected pixels for the N-1 interferograms using an implementation of the Minimum Cost Flow method (Costantini, 1998). The resulting phases are then integrated to obtain a set of phases, which are temporally ordered, in correspondence to the N images. An Atmospheric Phase Screen (APS) estimation follows, which makes use of known stable areas located in the observed scene. It is worth noting that the geometry and distribution of these areas strongly influences the quality of the APS estimates. Finally, the APS-cleaned phases are converted in Line-Of-Sight (LOS) displacements and geocoded, obtaining the two main

GBSAR products: the geocoded accumulated deformation maps and the geocoded deformation time series. Some specific aspects of D-GBSAR are briefly discussed below.

- **Density of the deformation measurements**. A major difference between C-GBSAR and D-GBSAR concerns the density of the available measurements. Even though this depends on the physical (dielectric) and geometric characteristics of the observed scene, the D-GBSAR data are usually much less dense than the C-GBSAR ones: in the worst cases a complete lack of measurements can occur. This limitation is similar to the one of satellite-based repeat-pass SAR interferometry, especially in X-band. This is illustrated in Figure 2, which compares the measurement density of Ku-band C-GBSAR and D-GBSAR. These results refer to the Canillo (Andorra) case study, which is discussed later in this paper. The D-GBSAR deformation measurements are very sparse: they cover few parts of the main street and the set of buildings located at the bottom right of the image. As it is discussed later, the measurement density is insufficient to cover the deformation area of interest and, for this reason, artificial CRs were deployed. By contrast, the C-GBSAR measurements offer a quite dense coverage, even on the forested and vegetated areas. The irregular measurement density visible in Figure 2 is mainly due to the lack of radar visibility of some parts of the scene.
- **Phase unwrapping**. This operation is critical in D-GBSAR applications for two main reasons. Firstly, the risk of unwrapping errors due to deformation grows with the time separation between GBSAR acquisitions (Monserrat et al., 2014): this requires a proper adjustment of the observation time interval. A non-interferometric approach to overcome this limitation has been recently proposed by Crosetto et al. (2013). A phase unwrapping procedure based on terrestrial laser scanner data is described in Wujanz et al. (2013). The second reason is related to the low measurement density, which characterizes D-GBSAR: a lower density implies greater distances between measurement pixels, which in turn makes more difficult the phase unwrapping.

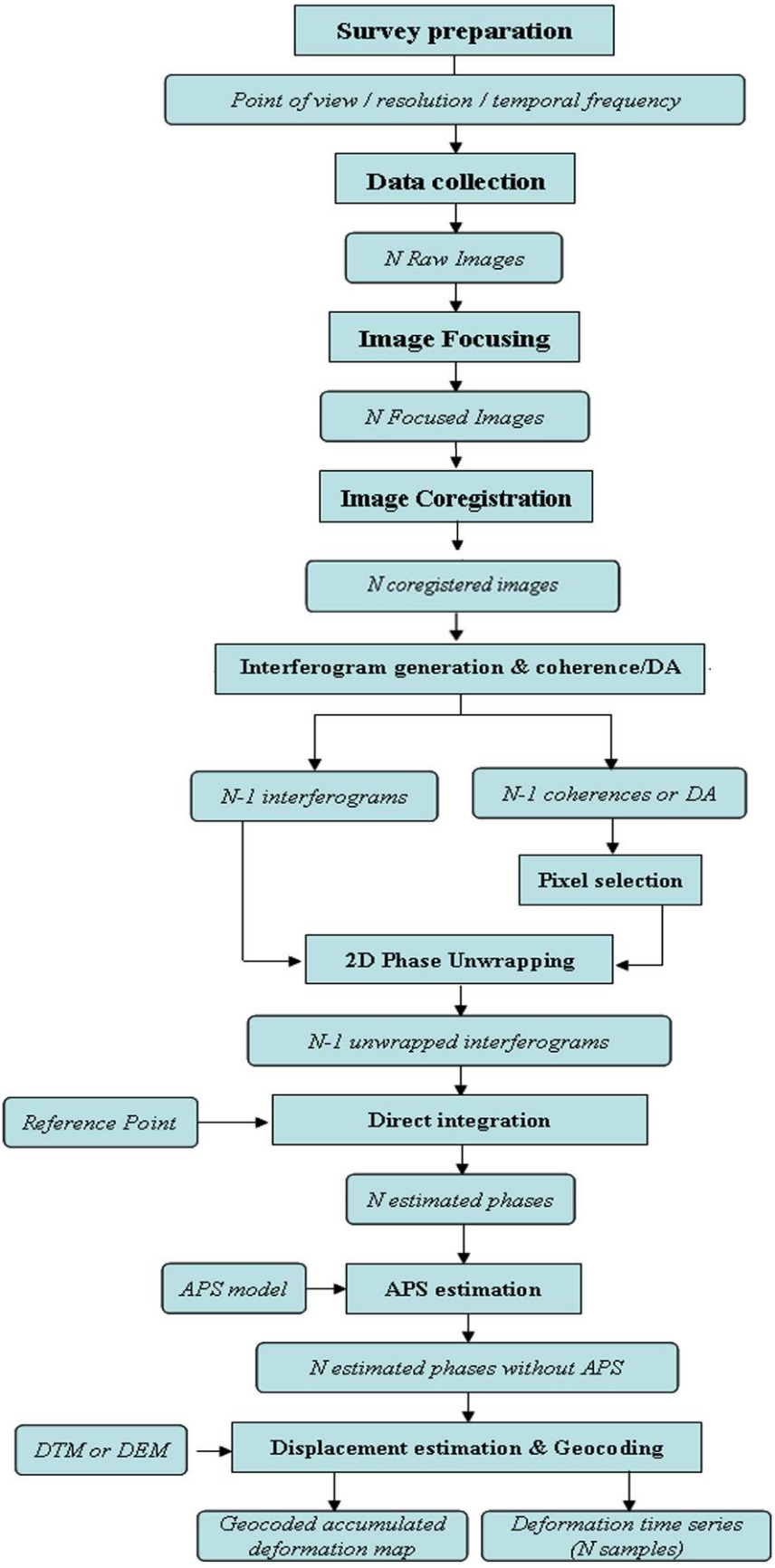

Figure 1. Flow chart of D-GBSAR data processing and analysis procedure used in this work.

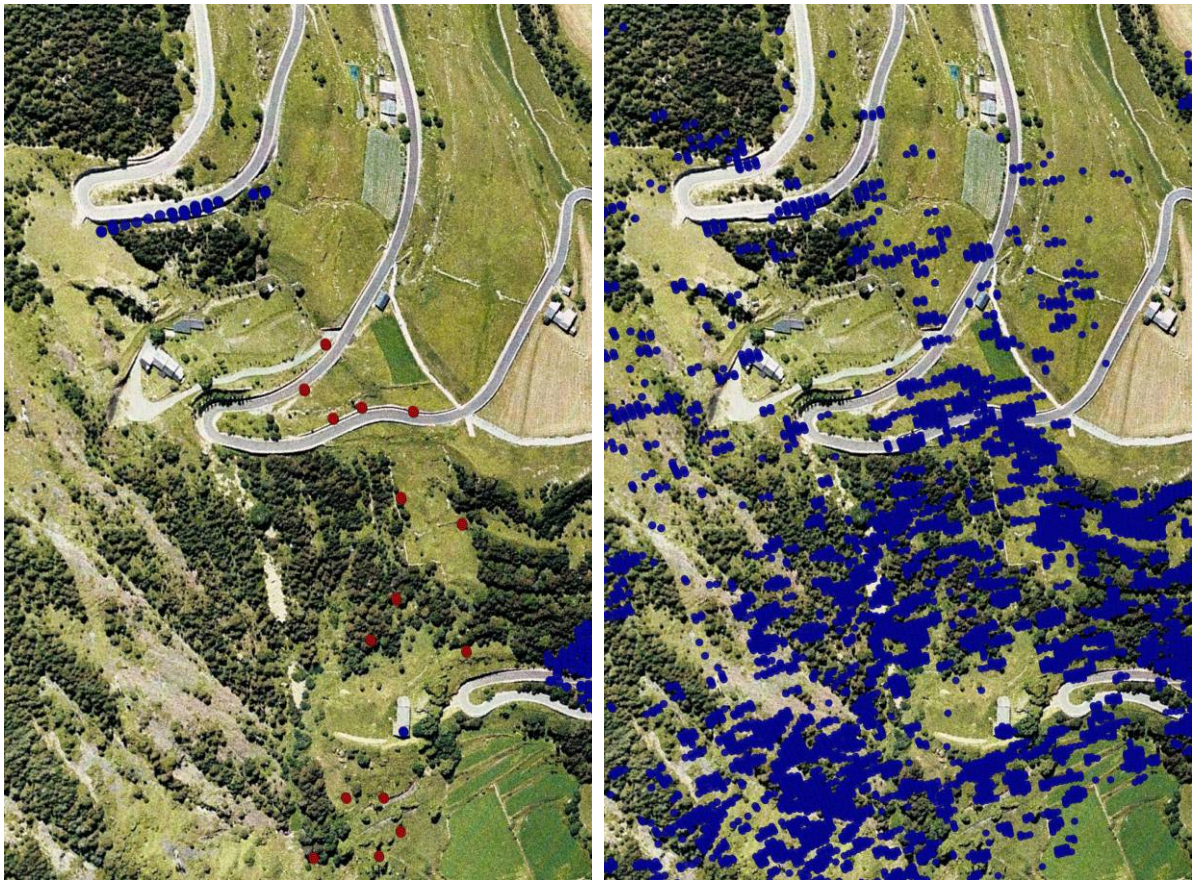

Figure 2. Comparison of the measurement density of Ku-band C-GBSAR, with time separation between image acquisitions of hours (right), and D-GBSAR, with time separation of some weeks (left). The red points correspond to 15 CRs. Depicted scene: “Forn de Canillo” landslide.

- **APS and repositioning effects**. The APS estimation represents a key step to properly derive the deformations. Note that the atmospheric effects, especially when combined with a low measurement density, can cause phase unwrapping errors. In addition, the D-GBSAR data may contain an additional phase component due to errors in the repositioning of the radar between different campaigns (Monserrat et al., 2014). These errors are usually non negligible, especially if “light positioning” is performed, e.g. by simply materializing the GBSAR location using some marks. Note that this is necessary in many practical cases, e.g. where a concrete base or any other precise mechanical positioning structure cannot be employed. The phase component due to repositioning errors is usually treated together with the APS because it has similar low spatial frequency characteristics.

3. First case study: urban area

This section describes the D-GBSAR deformation monitoring of an urban area: the village of Barberà de la Conca (Catalonia, Spain). This village has experienced deformations since 2011 that have caused cracks in the church and several buildings. Four D-GBSAR campaigns were

Figure 3. Photograph of the measured scene, Barberà de la Conca in the first case study, taken from the radar viewpoint. The radar with its two antennas is visible in the foreground.

performed (14/11/11, 19/12/11, 08/05/12 and 20/03/13), covering a total observation period of about 16 months. The radar was installed outside the village at an average distance of 500 m, see a photograph of the imaged scene in Figure 3. The data analysis was based on 10 SAR images for each campaign, from which four coherently averaged images were derived. A first important characteristic of this site concerns the measurement density: as it can be observed in Figure 4, over the observed scene there is a dense set of measurements, which cover a great number of buildings and structures. This was checked after the second campaign, proving the

Figure 4. Displacement maps of Barberà de la Conca between the first campaign (14/11/2011) and the campaigns of 19/12/2011 (a), 08/05/2012 (b) and 20/03/2013 (c). The blue polygons on the top indicate the stable areas.

feasibility of D-GBSAR monitoring without deploying CRs. A second key characteristic is a favourable geometry to estimate the APS: the deformation area is surrounded by stable areas,

see Figure 4a. Between the first two campaigns the displacements are imperceptible, see Figure 4a. However, from the third campaign they are clearly visible, see Figures 4b and 4c, and include two main deformation areas: the one in yellow to red colours, which indicate deformation values toward the radar up to 14.6 mm, and the one in light blue to blue colours, which indicates deformation values away from the radar up to -8.9 mm. These two areas are characterized by opposite slope aspects. Figure 5 shows the estimated deformation time series for a set of pixels moving toward the radar: it is perceptible that the deformations are stronger up to May 2012, while they reduce sensibly between May 2012 and March 2013.

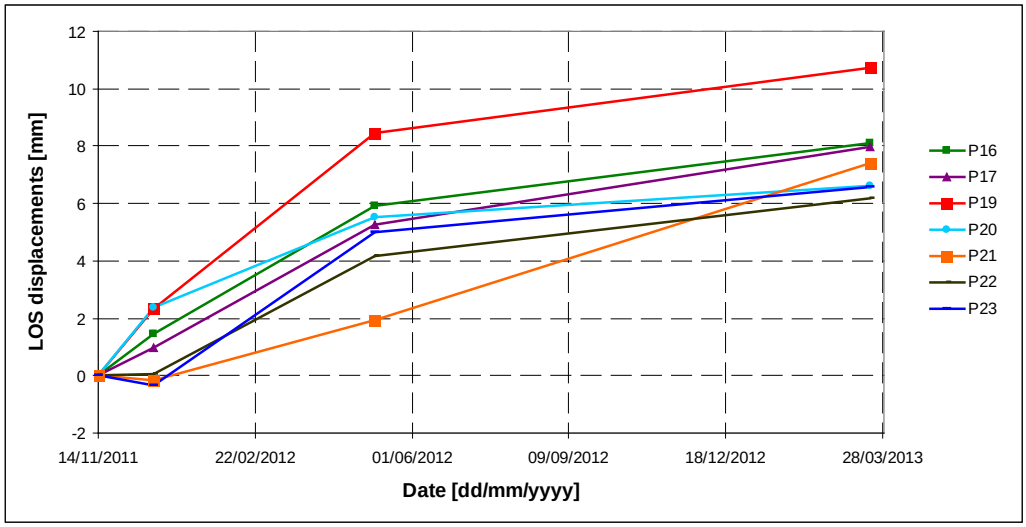

Figure 5. Estimated deformation time series for a set of pixels from the most active deformation area in Barberá de la Conca.

4. Second case study: rural area

This section describes the monitoring of the “Forn de Canillo” landslide, located near the village of Canillo (Andorra). The area of interest, seen from the radar viewpoint, is shown in Figure 6. As it is discussed in a previous section, see Figure 2, the D-GBSAR measurement density in this area is insufficient to cover the deformation phenomenon of interest. For this reason, 15 artificial CRs (Figure 7) were installed at each of the three D-GBSAR campaigns, which were carried out the 29/09/2009, 21/10/2009 and 25/11/2009. In this case we used a “light repositioning” based on marks painted on stones, walls, etc. The set of CRs is sufficient

to appropriately sample the deformation area of interest. However, the geometry and distribution of the measurements is weaker than in the previous case study and this influenced both the phase unwrapping and the APS estimation.

The D-GBSAR deformation map, which refers to the total observed period of 57 days, is shown in Figure 8. All movements observed in this scene are towards the radar. The maximum displacements value is 14 mm but, as shown in Figure 9, the CRs show a wide range of displacements, from almost zero to 14 mm. Carrying out a geomorphologic analysis and considering the displacements of the CRs, three different deformation areas were identified, see Figure 8 (Luzi et al., 2010). The area at the top was not moving between the first two campaigns and had moderate displacements in the following period. The strongest movements occur in the mid area. Note that there is a green point in this area which, most probably, is located out of the landslide body. Finally, the bottom area, which has lower slope values, shows slower displacements.

Figure 6. Photograph of the measured scene in the second case study, taken from the radar viewpoint. The blue circle highlights the main area of interest, which is located between 1000 and 1600 m from the radar.

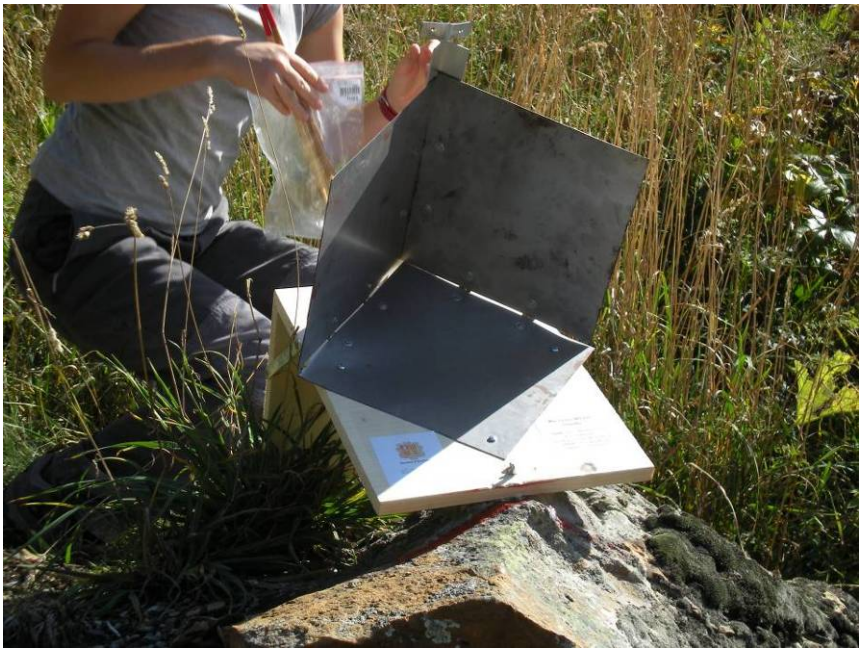

Figure 7. One of the 15 CRs deployed in the second case study, the “Forn de Canillo” landslide. The Corner Reflectors were installed and removed at each of the three measurement campaigns.

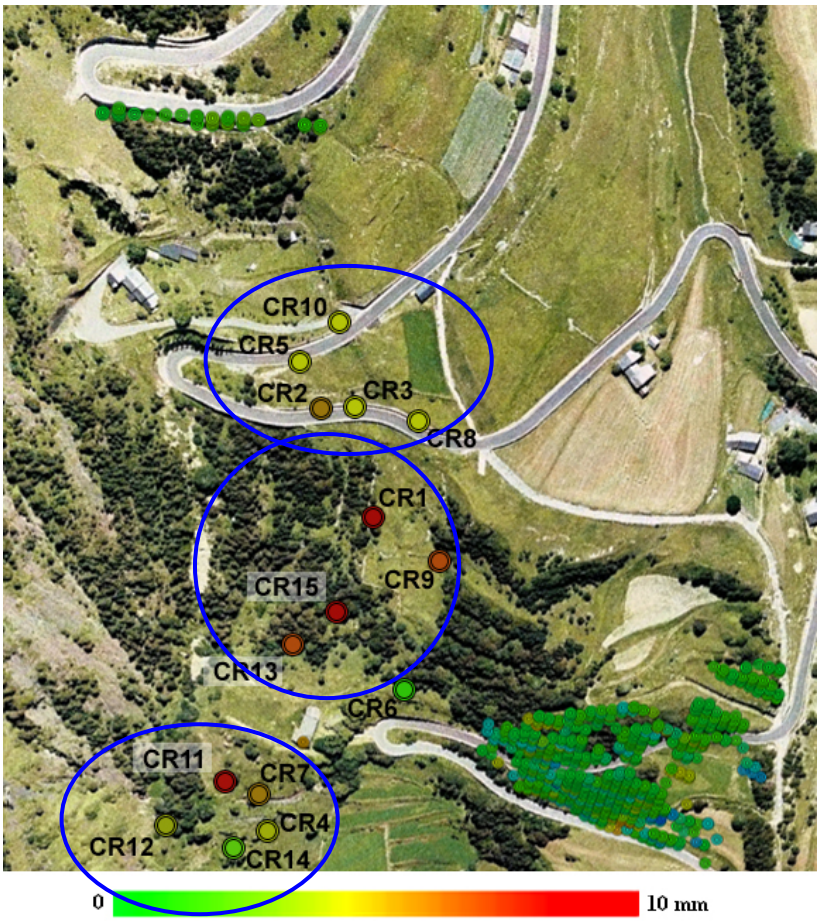

Figure 8. Displacement map of the “Forn de Canillo” landslide between the first (29/09/2009) and the last (25/11/2009) campaigns. The blue circles indicate three different deformation areas identified in the observed landslide.

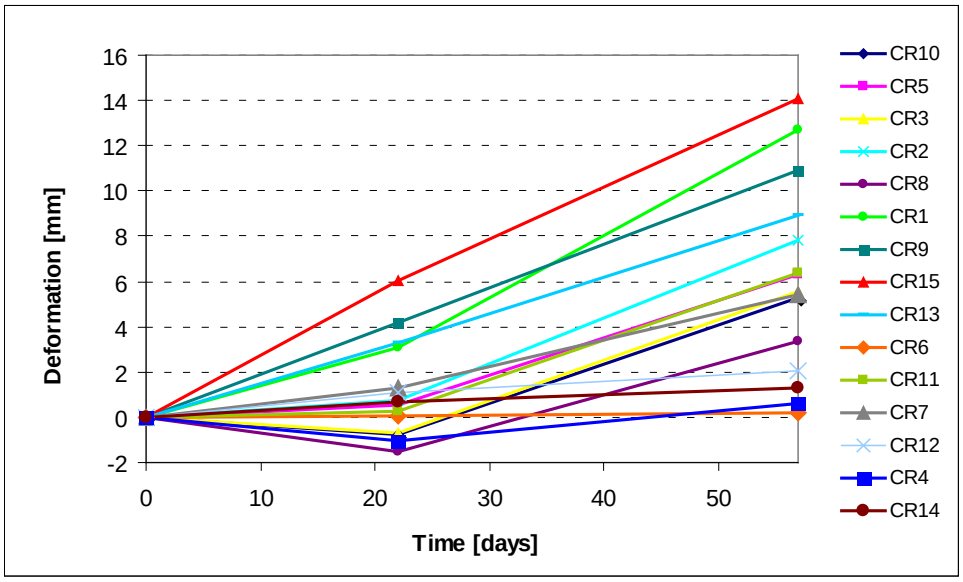

Figure 9. Estimated deformation time series for the 15 CRs deployed in the second case study, the "Forn de Canillo" landslide.

Conclusions

In this paper the deformation monitoring based on the discontinuous GBSAR (D-GBSAR) configuration has been addressed. This represents an acquisition mode that is useful to monitor slow deformation phenomena and that has been rarely described in the literature. It offers the advantage of reduced monitoring costs by using the same instrument over several sites. However, it requires a more complex data processing and, generally speaking, yields reduced measurement density, precision and reliability. The entire D-GBSAR data processing procedure implemented by the authors has been outlined, and the specific aspects of D-GBSAR have been discussed including: (i) the density of the deformation measurements, which can be a limiting factor for many D-GBSAR applications; (ii) the phase unwrapping, which can be critical for both the time separation between GBSAR acquisitions and the low measurement density of D-GBSAR measurements; and (iii) the atmospheric effects that are, in general, stronger in D-GBSAR than in the C-GBSAR data.

Two successful examples of D-GBSAR deformation monitoring have been described: the first case study concerns an urban area, while the second one involves a rural area. Both case

studies were monitored using a Ku-band GBSAR. The main outcomes of these case studies are:

- The urban case study represents a positive deformation monitoring example, which was derived in a fully remote mode, positioning the radar at a distance of 0.5 km. This aspect can be relevant for several applications, where the accessibility to the area of interest is difficult or impossible.
- A key characteristic of the urban case study is the high density of deformation measurements, which is sufficient to cover a great number of buildings and structures.
- A second fundamental characteristic of the urban case study is the favourable geometry to estimate the APS: the stable areas surround the deformation areas. This allowed us to properly separate the deformation and atmospheric phase components and hence correctly estimate the deformations.
- The rural case study represents a more complex deformation monitoring example: deformation measurements are not available in the main area of interest and 15 artificial CRs were installed to overcome this lack of measurements.
- It is worth noting that the monitoring was performed by installing and removing both the radar and the CRs at each of the three D-GBSAR campaigns. This represents the least invasive monitoring configuration.
- In both case studies, the obtained deformation maps and time series illustrate how a rich spatial and temporal description of a given deformation phenomenon can be obtained using D-GBSAR. In the urban case study, two main deformation areas have been found, while in the rural case study three parts of the monitored landslides have been identified.

Acknowledgements

This work has been partially funded by the Government of Catalonia, through the SAXA project (2010CTP00048) of the Comunitat de Treball dels Pirineus (www.ctp.org), and by the

Spanish Ministry of Science and Innovation, through the XLIDE project (IPT-2011-1287-370000) in the framework of the INNPACTO programme.

References

Barla, G., Antolini, F., Barla, M., Mensi, E., Piovano, G., 2010. Monitoring of the Beauregard landslide (Aosta Valley, Italy) using advanced and conventional techniques. Eng. Geol., 116, pp. 218-235.

Casagli, N., Farina, P., Leva, D., Nico, G., Tarchi, D. 2003. Ground-based SAR interferometry as a tool for landslide monitoring during emergencies. Proc. IGARSS 2003, vol. 4, pp. 2924-2926.

Casagli, N., Catani, F., Del Ventisette, C., Luzi, G., 2010. Monitoring, prediction, and early warning using ground-based radar interferometry. Landslides 7 (3), pp. 291–301.

Costantini, M., 1998. A novel phase unwrapping method based on network programming. IEEE Transactions on Geoscience and Remote Sensing, vol. 36, no. 3, pp. 813–821.

Crosetto, M., Monserrat, O., Luzi, G., Cuevas-Gonzalez, M., Devanthery, N., 2013. A Noninterferometric Procedure for Deformation Measurement Using GB-SAR Imagery. Geoscience and RS Letters, IEEE , 99, pp. 1

Farina, P., Leoni, L., Babboni, F., Coppi, F., Mayer, L., Coli, N., Thompson, C., 2012. Monitoring engineered and natural slopes by ground-based radar: methodology, data processing and case studies review. Proc. SHIRMS 2012, May 15-17, 2012 Sun City, South Africa.

Ferretti, A., Prati, C., Rocca, F., 2001. Permanent scatterers in SAR interferometry. IEEE TGRS, 39 (1), pp. 8-20.

Luzi, G., M. Pieraccini, D. Mecatti, L. Noferini, G. Macaluso, A. Galgaro, Atzeni, C., 2006. Advances in ground based microwave interferometry for landslide survey: a case study. International Journal of Remote Sensing, 27(12), pp. 2331 – 2350.

Luzi, G., Monserrat, O., Crosetto, M., Copons, R., Altimir, J., 2010. Ground-Based SAR interferometry applied to landslide monitoring in mountainous areas. Proceedings of the Mountain Risks conference, 24-26 November 2010a, Florence, Italy.

Mecatti, D., Macaluso, G., Barucci, A., Noferini, L., Pieraccini, M., Atzeni, C., 2010. Monitoring open-pit quarries by interferometric radar for safety purposes. Proc. of European Radar Conference (EuRAD), 30 September-1 October 2010, Paris, France, pp. 37-40.

Monserrat, O., 2012. Deformation measurement and monitoring with Ground-Based SAR. PhD thesis, Technical University of Catalonia, available on-line at www.ideg.cat.

Monserrat, O., Crosetto, M., Luzi, G., 2014. A review of ground-based SAR interferometry for deformation measurement. ISPRS Journal of Photogrammetry and Remote Sensing (submitted).

Noferini, L., Takayama, T., Mecatti, D., Macaluso, G., Luzi, G., Atzeni, C., 2008. Analysis of Ground-Based SAR data with diverse temporal baselines. IEEE TGRS 46 (6), pp. 1614–1623.

Noferini, L., Mecatti, D., Macaluso, G., Pieraccini, M., & Atzeni, C., 2009. Monitoring of Belvedere Glacier using a wide angle GB-SAR interferometer. Journal of Applied Geophysics, 68(2), pp. 289-293.

Noon, D., Harries, N., 2007. Slope Stability Radar for Managing Rock Fall Risks in Open Cut Mines, Proceeding of Large Open Pit Mining Conference Perth, WA, 10 - 11 September 2007.

Pieraccini, M., G. Luzi, D. Mecatti, M. Fratini, L. Noferini, L. Carissimi, G. Franchioni, C. Atzeni, 2004. Remote sensing of building structural displacements using a microwave interferometer with imaging capability, NDT & E International, 37(7),October 2004, pp. 545-550.

Pipia, L.; Fabregas, X.; Aguasca, A.; Lopez-Martinez, C., 2013. Polarimetric Temporal Analysis of Urban Environments With a Ground-Based SAR. IEEE TGRS, 51(4), pp. 2343-2360. doi: 10.1109/TGRS.2012.2211369.

Strozzi, T., Werner, C., Wiesmann, A., Wegmuller, U., 2012. Topography Mapping With a Portable Real-Aperture Radar Interferometer, IEEE Trans. Geosci. Remote Sens. Letters, vol. 9, Issue 2, 2012.

Tarchi, D., Ohlmer, E., Sieber, A.J., 1997. Monitoring of structural changes by radar interferometry. Journal of Research in Nondestructive Evaluation, 9 (4), pp. 213-225.

Tarchi, D., Rudolf, H., Luzi, G., Chiarantini, L., Coppo, P., Sieber, A.J., 1999. SAR interferometry for structural changes detection: A demonstration test on a dam. Proc. of IGARSS 1999, Hamburg, Germany, pp. 1522–1524.

Tarchi, D., Casagli, N., Fanti, R., Leva, D., Luzi, G., Pasuto, A., Pieraccini, M., Silvano, S., 2003a. Landslide monitoring by using ground-based SAR interferometry: an example of application. Engineering Geology, 68 (1–2), pp. 15–30.

Tarchi,D., Casagli, N., Moretti, S., Leva, D., Sieber, A.J., 2003b. Monitoring landslide displacements by using ground-based radar interferometry: Application to the Ruinon landslide in the Italian Alps, J. Geophys. Res., 108(10), pp. 1-14.

Tarchi, D., Antonello, G., Casagli, N., Farina, P., Fortuny-Guasch, J., Guerri, L., Leva, D., 2005. On the Use of Ground-Based SAR Interferometry for Slope Failure Early Warning: the Cortenova Rock Slide (Italy). Landslides: Risk Analysis and Sustainable Disaster Management, Proc. of the 1st General Assembly of the Int. Consortium on Landslides, Sassa, K. et al. (Eds.), Springer-Verlag, Berlin, Heidelberg.

Wujanz, D., Neitzel, F., Hebel, H.P., Linke, J., Busch, W. 2013. Terrestrial radar and laser scanning for deformation monitoring: first steps towards assisted radar scanning. ISPRS Annals, Volume II-5/W2, ISPRS Workshop Laser Scanning 2013, 11–13 November 2013, Antalya, Turkey.